Int J Adv Manuf Technol (2017) 88:3163–3173
DOI 10.1007/s00170-016-9027-0

ORIGINAL ARTICLE

Variable contour two-step warm extrusion forming of spur gear and the deformation behavior of $20Cr_2Ni_4A$ steel

Wei Wang[1,2] · **Jun Zhao**[1,2] · **Ruixue Zhai**[1,2] · **Rui Ma**[1,2]

Received: 25 February 2016 / Accepted: 6 June 2016 / Published online: 15 June 2016

Abstract The warm deformation behavior of $20Cr_2Ni_4A$ steel and the relative constitutive equation are ascertained to support the technical study. Factors that influence the warm extrusion of spur gear are analyzed by using the numerical simulation method. Among the various influencing factors, the lubricating condition, entrance angle, and initial blank size are the crucial factors. Spur gears with a good quality can be one-step formed by warm extrusion under a good lubricating condition (friction factor less than 0.3). Nevertheless, this kind of lubricating condition is very hard to be achieved in a real production environment. "Variable contour two-step warm extrusion" is proposed, in order to obtain a good forming result in a poor lubricating condition. Pre-extrusion is firstly implemented by a die which contour is enlarged from the final-toothed contour for the tooth forming, and then the workpiece is turned around to implement the finish extrusion by a die with the final-toothed contour for insufficient section compensation and tooth sizing. Accuracy of the finished gear obtained through this process is tested; the maximum mean error of single tooth is 15.5 μm.

Keywords Spur gear · Variable contour · Warm extrusion · $20Cr_2Ni_4A$ steel · Deformation behavior

✉ Jun Zhao
wangweicaijia@ysu.edu.cn; zhaojun@ysu.edu.cn

[1] Key Laboratory of Advanced Forging and Stamping Technology and Science (Yanshan University), Ministry of Education of China, Qinhuangdao 066004, People's Republic of China

[2] School of Mechanical Engineering, Yanshan University, Qinhuangdao 066004, People's Republic of China

1 Introduction

Spur gear manufacturing is mainly through the metal cutting in industrial production; there are some inevitable disadvantages, material waste, low efficiency, and high cost. Especially, as a result of metal fibers being cut off, the comprehensive mechanical property is weakened. With the aggravation of energy crisis and resource depletion, a new technology is urgently desired to be developed to replace the traditional process.

Forging of spur gears is the pioneer and has been researched extensively. The spur gears and spines by closed die forging are proposed by Abdul and Dean [1]. Divided flow method for spur gears forging is explored by Kondo and Ohga [2], in order to reduce the forming force. The spur gear forging by an inside relief die is studied by Choi and Choi [3]. Four alternatives of die designs are discussed by Cai et al. [4] to reduce the forming force and improve the forming quality. In order to lower the load of the cold forging of the spur gears, the punch and bottom end faces are changed by Hu et al. [5]. A radial rigid-parallel-motive flow mode is proposed by Hu et al. [6]; based on this mode, a two-step forging process of spur gear is proposed. The feasibility for hot forging by using lower strength material is studied by Cheng et al. [7]; a spur gear is formed by using the proposed method. But the service life of die and the precision of formed gear are not discussed. A two-step forging process of spur gear is developed by Yang et al. [8] to reduce the forming load.

Throughout its development history, it is clear that a key constraint of the gear forging is the contradictory relationship existing between the forming load and the forming precision. This is due to the load direction perpendicular to the metal flow direction during spur gear forging, which results in the gear teeth corners being filled difficultly or the big forming load being applied leads to the service life of dies being

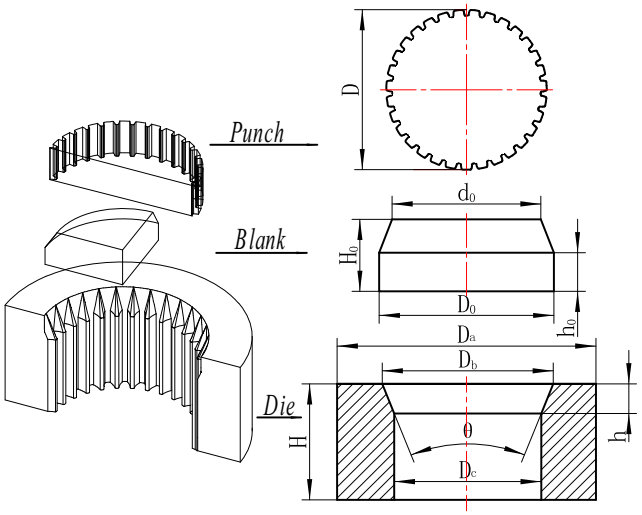

Fig. 1 Model of warm extrusion forming of spur gear

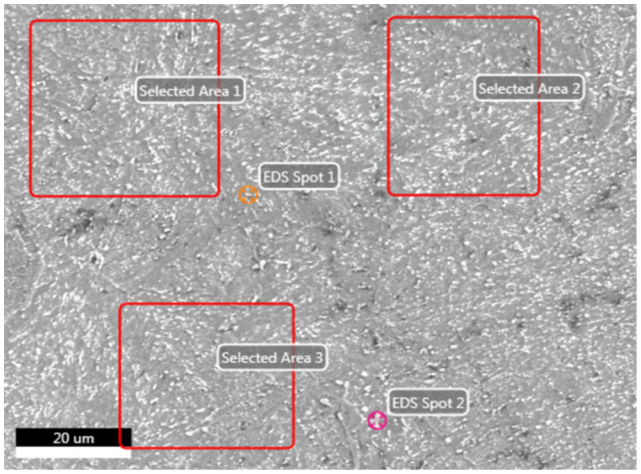

Fig. 3 Detecting areas and spots

shorted. This also is the reason why the bevel gears can be easily formed [9–11], but almost all of the existing gear forging technologies could not be successfully applied in an industry scale production.

In recent years, gear forming by rolling technology is explored by Neugebauer et al. [12, 13]. And the rolling technology for forming shaft with thread and spline is proposed by Zhang and Zhao [14]. The principle is similar to rotary forging of bevel gears [15, 16]. Integral forming is replaced by the continuously local forming, so that the forming force is observably reduced. Nevertheless, one problem existing in this process is how to accurately divide gear teeth. The free rolling often generates gear clutters and tooth profile deviation, while the forcing rolling needs strict tools and equipment to ensure precision of the formed gears. Furthermore, another problem is the low production efficiency.

The open-die extrusion is one forming technology with lower forming load, also applied to manufacture the pinions and spline shafts. The principle of manufacturing spline shaft by open-die extrusion is analyzed by Li et al. [17], and a tooth-divided flow method is presented. The cold extrusion process of helical pinion gear is researched by Jeong et al. [18]; minimum distance analysis is used in FE simulation to design the shape of die and initial billet for the dimensional accuracy improvement. The three-dimensional velocity field of cold extrusion of trapezium spline is analyzed by Yuan [19], and the simulation is implemented by using the Deform-3D software. Solid or hollow spur gears by cold forward extrusion are studied by Song and Im [20]; the applicability of the automated process design system is confirmed through experiments. A CFAQT process is proposed by Hu et al. [21], by using this process the spline extrusions successfully. Through finite element method and artificial neural network to predict the extrusion load of extrusion of gear-like profiles is researched by Bingöl et al. [22]. An extrusion process for manufacturing helical gear is presented by Jung et al. [23]; the process is composed primarily of extruding a billet to a spur gear and then twisting the previous spur gear extruded to a helical gear.

The warm extrusion technology is a combination of the warm forming and the extrusion process, which is more applicable for manufacturing large module gears using low forming load. Furthermore, the tools of warm extrusion are simple and highly reliable. In this paper, the feasibility of the warm extrusion for manufacturing spur gears is investigated through numerical simulation and experiments, and the improved process "variable contour two-step warm extrusion" is presented. In the mean time, the warm deformation behavior of $20Cr_2Ni_4A$ steel (Chinese grade) is ascertained to support the technical study.

2 Process model and principle

The model of warm extrusion forming of spur gears is illustrated in Fig. 1; half of the punch and die and one quarter of the blank are shown for clarity. The punch is designed as a gear-like structure in order to avoid a big burr using a round punch or a big forming force using a whole tooth punch. The die

(I) Gear tooth dividing (II) Gear tooth forming (III) Truing

Fig. 2 Forming principle

Table 1 Chemical component of $20Cr_2Ni_4A$ steel

Element	C	Si	Mn	Cr	Ni	S	P	Fe
wt.%	0.17 ~ 0.23	0.16	0.48	1.48	3.12	≤0.03	≤0.03	Bal.

includes an entrance section and a forming section. The entrance section has a correlative entrance angle (θ) and height (h); the forming section has a toothed contour. In the extrusion process, besides the lateral extrusion, the surface of the blank also generates backward extrusion, so the initial blank is chamfered in its head, which is easily obtained by forging.

Figure 2 shows the forming principle which consists of three stages. In stage I, the blank bottom is divided by the entrance section. In stage II, the blank bottom is formed to the gear teeth shape, and the blank top is divided continually. In stage III, the blank continues going downward until its breaking away from the die.

3 Warm deformation behavior of $20Cr_2Ni_4A$ steel

3.1 Materials and compression tests

$20Cr_2Ni_4A$ steel is a kind of high-quality alloy steel able to provide excellent comprehensive mechanical performance, with its prominent hardenability and obdurability. $20Cr_2Ni_4A$ steel is widely used in manufacturing transmission gears in both military and civil. There are very few research reports of the deformation behavior of the $20Cr_2Ni_4A$ steel. Therefore, the deformation behavior of the $20Cr_2Ni_4A$ steel is investigated, in order to increase the accuracy of the numerical simulation and provide contributions to the process parameter determination. The chemical components of the $20Cr_2Ni_4A$ steel are detected by SEM-EDS analysis with a HITACHI 3400N. Figure 3 shows the detecting areas and spots, and Table 1 lists the detecting results.

The compression tests are implemented on a Gleeble-3500 thermal simulation machine at different deformation

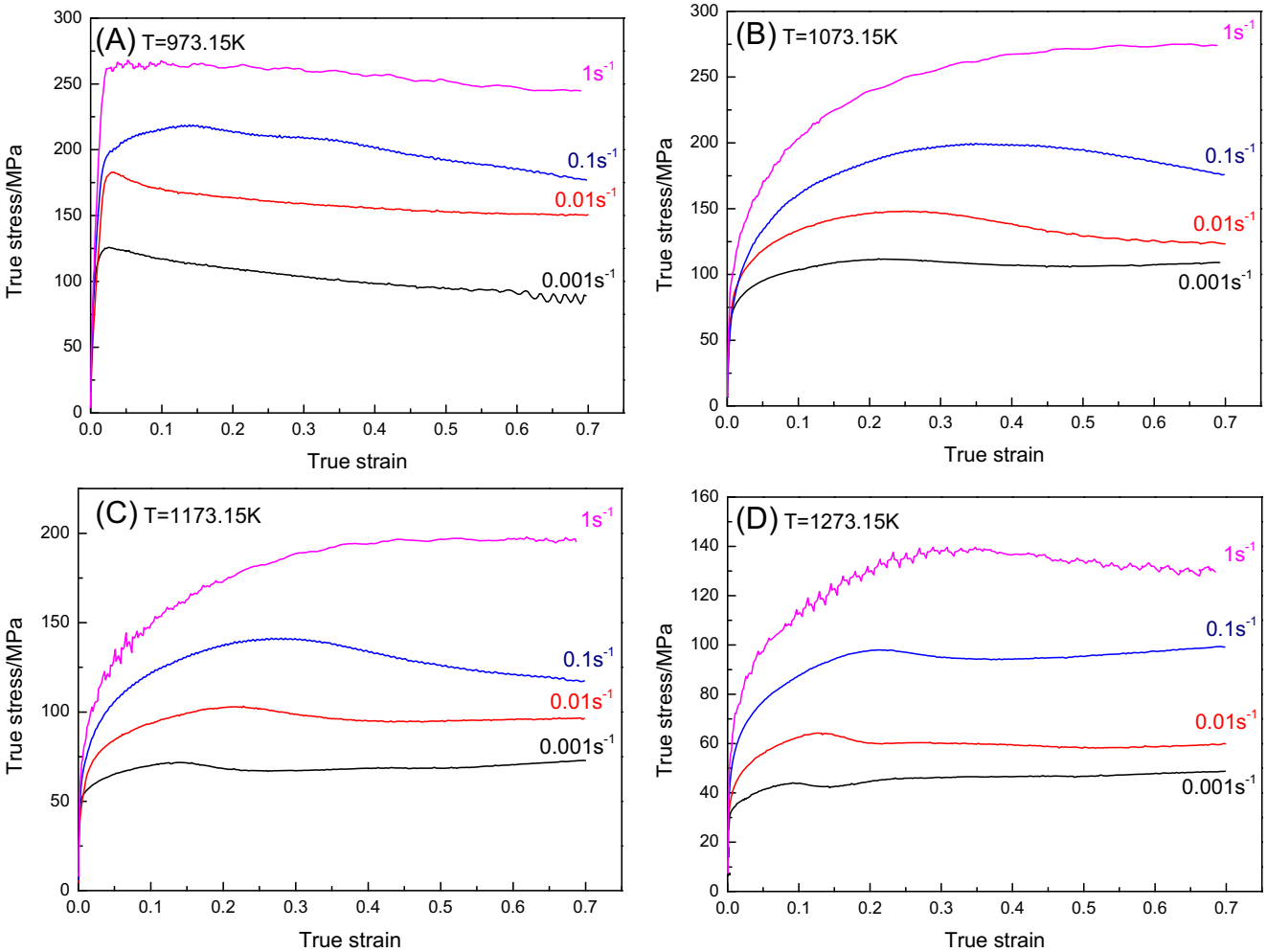

Fig. 4 True stress-strain curves of $20Cr_2Ni_4A$ steel under different temperatures and strain rates

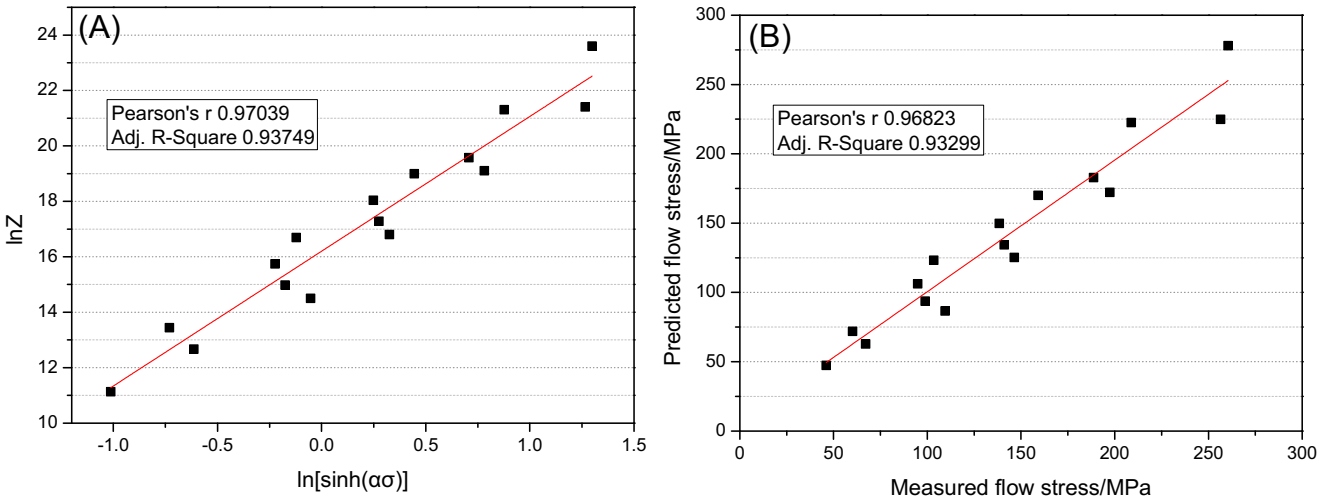

Fig. 5 **a** Plot of ln$Z$ versus ln[sinh($\alpha\sigma$)] and **b** comparison between the predicted and experimental $\sigma_{0.3}$ values

temperatures of 973.15, 1073.15, 1173.15, and 1273.15 K, with strain rates of 0.001, 0.01, 0.1, and 1 s^{-1}. The specimen size is 8 mm in diameter and 12 mm in height. Each surface of the specimen is covered with the tantalum foil to minimize friction. The specimens are initially heated to the deformation temperature at 10 K/s and then are held for 3 min to homogenize the temperature. Reduction rate in the height is 50 %, namely the true strain reached to 0.7.

3.2 Flow behavior and constitutive equation

Based on the isothermal compression tests, the true stress-strain curves of the $20Cr_2Ni_4A$ steel are plotted, as shown in Fig. 4. The deformation behavior of the $20Cr_2Ni_4A$ steel is coincident with the typical rules of the alloy steel [24, 25]. The true stress-strain curves integrally offset to the low stress area with the increase of the deformation temperature or the decrease of the strain rate. However, this material also has its specific feature, the softening mechanism rapidly gaining to the upper hand at 973.15 K (Fig. 4a). According to the iron-carbon phase diagram, the eutectoid transformation temperature of carbon steel is 1000.15 K. The addition of alloy elements in carbon steel will cause the change of the transformation temperature. Especially, the addition of Ni element will expand the austenite phase region which leads to the decrease of eutectoid transformation temperature. The eutectoid transformation temperature of $20Cr_2Ni_4A$ steel could be 973.15 K. That might be the reason why Fig. 4a is different from the others. The Arrhenius-type constitutive equation is adopted to describe the warm deformation behavior of $20Cr_2Ni_4A$ steel. In addition, influence of the forming temperature and strain rate on the deformation behavior could be described by Zener-Hollomon parameter Z, as shown in Eqs. (1–3).

Table 2 Coefficients of the polynomial functions

n		α		Q		ln$A$	
B_0	7.99362	C_0	0.01048	D_0	0.01048	E_0	45.66636
B_1	−22.504	C_1	−0.02547	D_1	−0.02547	E_1	−305.061
B_2	69.85795	C_2	0.08463	D_2	0.08463	E_2	1343.97
B_3	−112.157	C_3	−0.11925	D_3	−0.11925	E_3	−3115.91
B_4	87.26999	C_4	0.05856	D_4	0.05856	E_4	3626.527
B_5	−23.0135	C_5	0.0042	D_5	0.0042	E_5	−1669.38

$$\varepsilon = \mathrm{A}\,\mathrm{F}(\sigma)\exp\left(-Q\Big/\mathrm{RT}\right) \tag{1}$$

$$\text{where}\, F(\sigma) = \begin{cases} \sigma^{n_1} & \alpha\sigma < 0.8 \\ \exp(\beta\sigma) & \alpha\sigma > 1.2 \\ [\sinh(\alpha\sigma)]^n & \text{for all } \sigma \end{cases} \tag{2}$$

$$Z = \dot{\varepsilon}\exp\left(Q\Big/RT\right) \tag{3}$$

Table 3 Detailed parameters of FE model

Parameter	Tooth number	Modules	Tooth thickness	Material	Die temperature	λ_1	λ_2
Value	31	2	20 mm	$20Cr_2Ni_4A$	473.15 K	5 N/(s · mm · C)	0.02 N/(s · mm · C)

λ_1 is the heat transfer coefficient between the blank and the die.
λ_2 is the convection coefficient to environment.

Table 4 Factors and levels

Factor	Level			
	1	2	3	4
Height of straight section (mm)	5	8	10	15
Entrance angle θ (°)	20	36	52	78
Forming temperature (K)	973.15	1073.15	1173.15	1273.15
Friction factor	0.2	0.3	0.5	0.7
Extrusion speed ($mm \cdot s^{-1}$)	10	20	30	40

Where $\dot{\varepsilon}$ is the strain rate (s^{-1}), σ is the flow stress (MPa), Q is the activation energy ($J \cdot mol^{-1}$), R is the gas constant ($R = 8.314\ J \cdot mol^{-1} \cdot K^{-1}$), T is the absolute temperature, and A, n_1, α, n, and β ($\beta = \alpha n_1$) are material constants.

The material constants are resolved using the following mathematical method. The average slope of linear fitting curves of $[\ln\sigma - \ln\dot{\varepsilon}]$ under different deformation temperatures is accepted as n_1. The average slope of linear fitting curves of $[\sigma - \ln\dot{\varepsilon}]$ under different deformation temperatures is accepted as β, and then α can be solved by $\alpha = \beta/n_1$. The average slope of linear fitting curves of $[\ln[\sinh(\alpha\sigma)] - \ln\dot{\varepsilon}]$ is accepted as n. The average slope of linear fitting curves of $[1000/T - \ln[\sinh(\alpha\sigma)]]$ under different strain rates is accepted as $Q/(Rn)$, then Q ($kJ \cdot mol^{-1}$) can be solved. At last, the intercept of linear fitting curve of $[\ln[\sinh(\alpha\sigma)] - \ln Z]$ is accepted as $\ln A$, then A can be solved. When the above mathematical method is used for evaluation at the true strain of 0.3 ($\sigma_{0.3}$), the values of the material constants are as follows: $n_1 = 7.0403$, $\alpha = 7.7166 \times 10^{-3} MPa^{-1}$, $n = 5.1480$, $Q = 190.96\ kJ \cdot mol^{-1}$, and $A = 1.0859 \times 10^7\ s^{-1}$. The Arrhenius-type constitutive equation with the Zener-Hollomon parameter for $20Cr_2Ni_4A$ steel at $\sigma_{0.3}$ could be expressed as follows:

$$\begin{cases} \sigma = 129.5906 \ln\left\{ \left(\dfrac{Z}{1.0859 \times 10^7}\right)^{1/5.148} + \left[\left(\dfrac{Z}{1.0859 \times 10^7}\right)^{2/5.148} + 1 \right]^{1/2} \right\} \\ Z = \dot{\varepsilon} \exp\left(\dfrac{190.96 \times 10^3}{8.314T}\right) \end{cases} \tag{4}$$

R^2 of the plot of $\ln Z$ versus $\ln[\sinh(\alpha\sigma)]$ is 0.937. R^2 of the predicted and the experimental values of $\sigma_{0.3}$ is 0.933, as shown in Fig. 5. It reveals that the predicted data from the above constitutive equation has a higher accuracy.

Since influence of the strain on the deformation behavior is not considered in Eq. (4), material constants (A, α, n, and Q) are deduced by using the abovementioned method at different strain values ranging from 0.05 to 0.7 with an interval of 0.05. The values of the constants (A, α, n, and Q) can be described by the fifth-order polynomial functions, as shown in Eq. (5). The coefficients of these polynomial functions are listed in Table 2.

$$\begin{cases} n = B_0 + B_1\varepsilon + B_2\varepsilon^2 + B_3\varepsilon^3 + B_4\varepsilon^4 + B_5\varepsilon^5 \\ \alpha = C_0 + C_1\varepsilon + C_2\varepsilon^2 + C_3\varepsilon^3 + C_4\varepsilon^4 + C_5\varepsilon^5 \\ Q = D_0 + D_1\varepsilon + D_2\varepsilon^2 + D_3\varepsilon^3 + D_4\varepsilon^4 + D_5\varepsilon^5 \\ \ln A = E_0 + E_1\varepsilon + E_2\varepsilon^2 + E_3\varepsilon^3 + E_4\varepsilon^4 + E_5\varepsilon^5 \end{cases} \tag{5}$$

4 Analysis of influence factors

4.1 FE model and experimental design

The deformation behavior of $20Cr_2Ni_4A$ steel is imported into commercial finite element analysis software DEFORM-3D.

Table 5 $L_{16}(4^5)$ orthogonal array

Scheme	Height of straight section (mm)	Entrance angle θ (°)	Forming temperature (K)	Friction factor	Extrusion speed ($mm \cdot s^{-1}$)
1	5	20	973.15	0.2	10
2	5	36	1073.15	0.3	20
3	5	52	1173.15	0.5	30
4	5	78	1273.15	0.7	40
5	8	20	1073.15	0.5	40
6	8	36	973.15	0.7	30
7	8	52	1273.15	0.2	20
8	8	78	1173.15	0.3	10
9	10	20	1173.15	0.7	20
10	10	36	1273.15	0.5	10
11	10	52	973.15	0.3	40
12	10	78	1073.15	0.2	30
13	15	20	1273.15	0.3	30
14	15	36	1173.15	0.2	40
15	15	52	1073.15	0.7	10
16	15	78	973.15	0.5	20

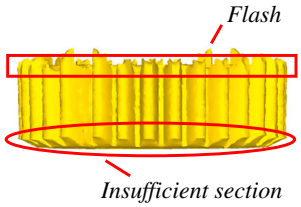

(A) Forming result in poor lubricating condition

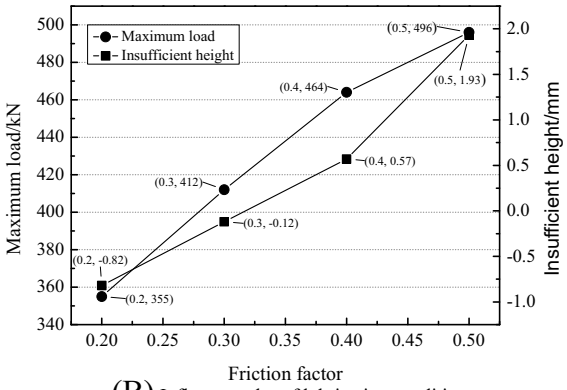

(B) Influence rules of lubricating condition

Fig. 6 Effects of lubricating condition

Base on DEFORM-3D with rigid-plastic model and shear friction model ($\tau_f = mk$), the FE model of the warm extrusion is established to explore the influencing factors on the forming quality. The detailed parameters of the FE model are listed in Table 3. In essence, one single tooth is enough to reflect the forming results. For a better clarity, eight teeth are chosen in the FE model. Element type, tetrahedron; element number, 50, 000; node number, 11,249; and min edge length, 0.4617 mm.

The foreseeable factors influencing the forming quality include initial blank size, entrance angle of die, friction factor, extrusion speed, and forming temperature. Four levels are set up for each individual factor (as listed in Table 4) to constitute the $L_{16}(4^5)$ orthogonal array (as listed in Table 5). Additionally, the initial blank size is determined by the equal volume principle and the height of the straight section (h_0) is determined as a variable.

4.2 Results and discussion

Through the orthogonal experiment, the lubricating condition, entrance angle, and initial blank size are determined as the crucial factors; the forming temperature and extrusion speed are not the crucial factors for forming results. However, the experimental results in the orthogonal array exist different forming defects. Such as insufficient section, material accumulation, and defect section. So it is difficult to make quantitative analysis through the orthogonal experiment results. Therefore, the quantitative analysis of each crucial factor is investigated by using the single factor experiment.

1. Effects of lubricating condition

The most significant factor influencing on the forming quality is the lubricating condition. When the friction factor is greater than 0.5, all of the forming results are not ideal. Because the metal material backward flows seriously, the velocity field is unbalanced during the extrusion process, which results in the insufficient section formed at the bottom of the workpiece, and the flashes are formed at the top of the workpiece, as shown in Fig. 6a.

Figure 6b shows the influence rules of the lubricating condition on the height of the insufficient section and the maximum forming load. The friction factor is set up from 0.2 to 0.5 at an interval of 0.1, with the fixed parameters: entrance angle at 36°, height of straight section at 10 mm, forming temperature at

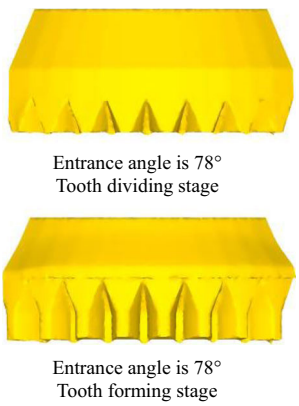

(A) Material accumulation

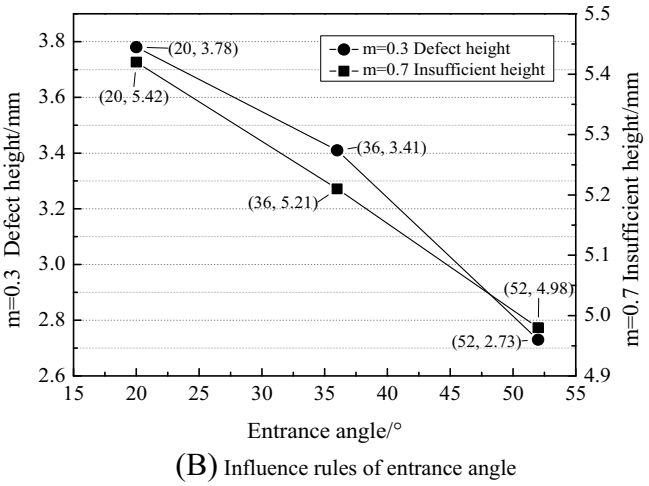

(B) Influence rules of entrance angle

Fig. 7 Effects of entrance angle on forming results

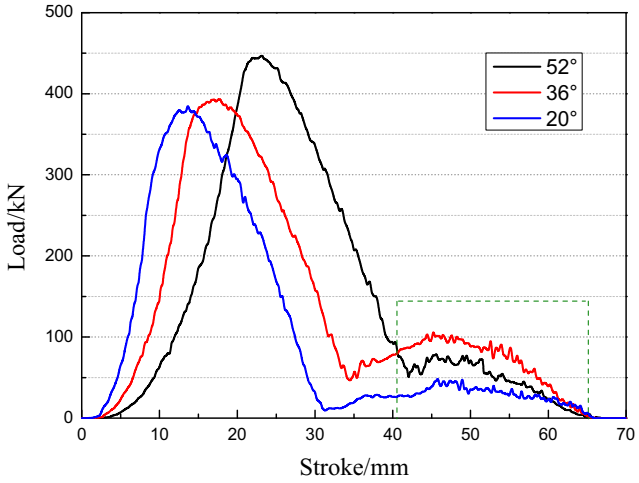

Fig. 8 Effects of entrance angle on forming load

1073.15 K, and extrusion speed at 10 mm·s^{-1}. It indicates the better lubricating condition with the better forming quality and the smaller forming load. When the lubricating condition is very good, the addendum elongates along the extrusion direction. This is because the contour of the entrance section gradually decreases; the blank generates the forward extrusion in the gear tooth dividing stage in good lubricating condition, but the forward extrusion degree is limited.

2. Effects of entrance angle

The second significant factor is the entrance angle of the die. If the entrance angle is too large, the blank cannot be divided sufficiently which lead to the material accumulation in the gear tooth forming stage, as shown in Fig. 7a.

Figure 7b shows the influence rules of the entrance angle on the height of the insufficient section in a poor lubrication (friction factor 0.7), and the influence rules on the height of the defect section in a good lubrication (friction factor 0.3). An illustration of the defect section is shown in Fig. 9a. The entrance angle is set up at 20°, 36°, and 52°, with the fixed parameters: friction factor at 0.3, height of straight section at 10 mm, forming temperature at 1073.15 K, and extrusion speed at 10 mm·s^{-1}. It reveals that on the premise of no material accumulation, both heights of the insufficient section and the defect section decrease with the increases of the entrance angle. It should be noted that although the heights of the insufficient section decreases with the increases of the entrance angle, the effect is not significant (5.42 mm at 20°, 5.21 mm at 36°, and 4.98 mm at 52°). However, the larger entrance angle leads to the increase of forming load in the gear tooth dividing stage, as shown in Fig. 8. When the entrance angle is 52°, the maximum forming load is significantly larger, that is harmful to die life. In addition, when the entrance angle is 36°, the forming load of the truing stage is higher than others (the dotted area in Fig. 8). It means that the contact between the workpiece and the die is better, namely, the gear teeth have a better forming effect. So the entrance angle at 36° is a more reasonable choice.

3. Effects of initial blank size

If process parameters are set up improperly, the defect section will be generated at the top of the blank. This defect will be worse if the straight section is too short (Fig. 9a). On the contrary, if the straight section is too long, the burr will be formed by non-filling materials (Fig. 9b).

Fig. 9 Effects of initial blank size

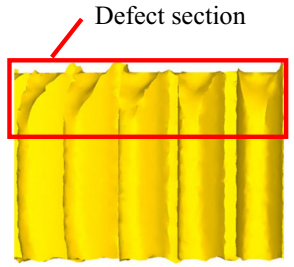

(A) Straight section 5mm

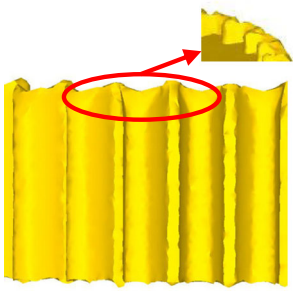

(B) Straight section 15mm

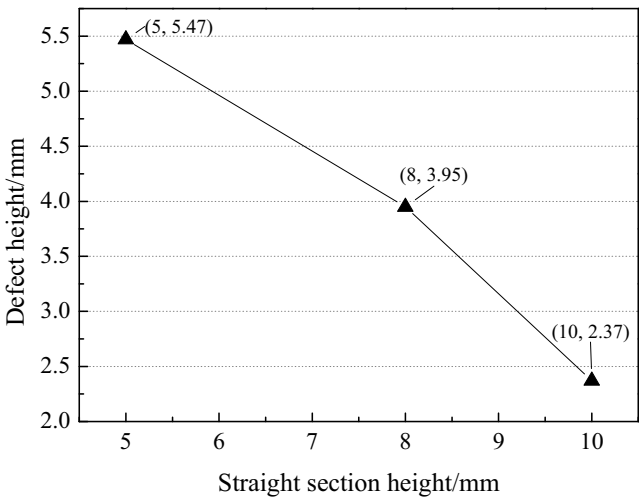

(C) Influence rules of straight section height

Table 6 Experimental schemes

Scheme	Height of straight section (mm)	Entrance angle θ (°)	Forming temperature (K)	Lubricant	Extrusion speed (mm · s^{-1})
1	10	36	1023.15 ~ 1073.15	Oil-base graphite	10
2	10	36	1023.15 ~ 1073.15	Water-base graphite	10
3	10	36	1023.15 ~ 1073.15	Lead oxide	10

Figure 9c shows the influence of the initial blank size on the defect section. The height of the straight section is set up at 5, 8, 10, and 15 mm, with the fixed parameters: entrance angle at 36°, friction factor at 0.3, forming temperature at 1073.15 K, and extrusion speed at 10 mm · s^{-1}. It can be observed that the longer straight section results in the shorter defect section and better forming quality. Even so, the burr should be avoided by selecting a reasonable initial blank size.

4.3 Preliminary experiment

Through the above analysis, the optimized parameters of three crucial factors are ascertained, friction factor at 0.3, entrance angle at 36°, and straight section at 10 mm. The forming temperature and the extrusion speed are not the crucial factors for forming results. The forming temperature is set as 1073.15 K; the reason for this choice is that the metal fluidity is good but the oxidation is not serious. According to the parameters of experimental equipment, the extrusion speed is set as 10 mm · s^{-1}. The experimental schemes are listed in Table 6. Because of the temperature fluctuation, the experimental heating temperature is limited to 1048.15 ± 25 K; the maximum temperature does not exceed 1073.15 K in the experiment process. The experimental equipment is YA-315T hydraulic press, the heating equipment is GP-60 ultra-audio-frequency induction heater. Preheating temperature on the die is 473.15 ~ 523.15 K. The experimental material is $20Cr_2Ni_4A$ steel. Figure 10 shows the initial blank, the die, and the experimental samples. Although the lubrication of the lead oxide is more suitable for the warm extrusion of spur gear, the forming quality still cannot achieve the level when the friction factor is less than 0.3. The insufficient section generates at the bottom of the workpiece, and there still are underfilling teeth.

Due to the complex contact surfaces between the blank and the die, the good lubricating condition is extremely difficult to achieve. A greedy pursuit of good lubricating condition will certainly bring forward rigorous demands on the surface quality of the die and the selection of lubricants, which will result in an increased production cost. In addition, the lubricating condition will certainly become worse with the continued production. Therefore, it is a significant subject that the good quality spur gears can also be formed in a poor lubricating condition.

5 Variable contour two-step warm extrusion

It is learnt from the preliminary experiments that the good quality spur gears cannot be formed by one-step warm extrusion, due to the restriction from the lubrication. In order to obtain the good forming results in a poor lubricating condition, the forming process is modified into variable contour two-step warm extrusion. Firstly, pre-extrusion is implemented by a die which the contour of the forming section is enlarged from the final-toothed contour. The formed spur gear is

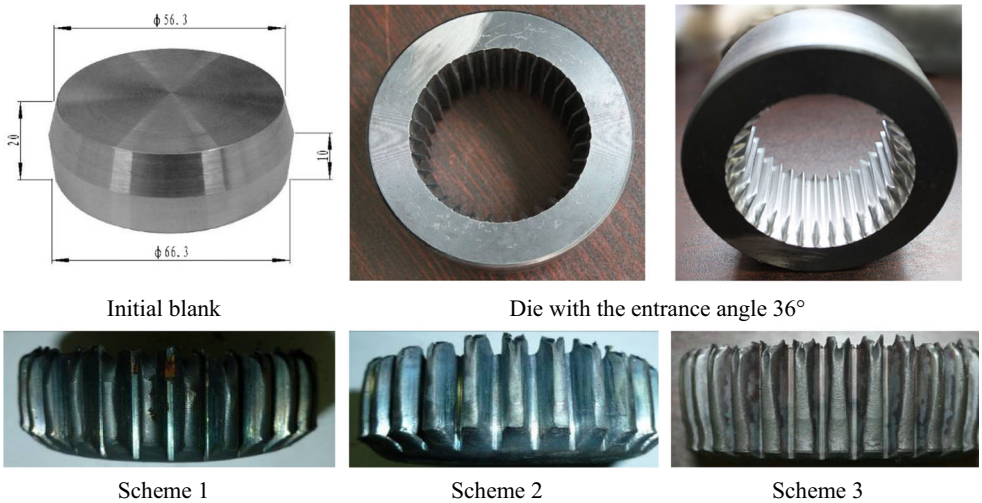

Fig. 10 Initial blank, die, and experimental samples

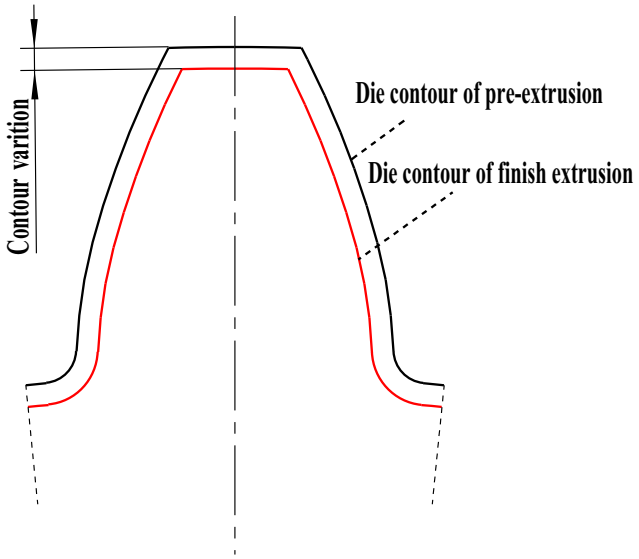

Fig. 11 Diagram of die contour of pre-extrusion and finish extrusion

allowed to have the insufficient section after pre-extrusion. And then, the workpiece is turned around to implement the finish extrusion by a die with the final-toothed contour. Figure 11 shows a diagram of die contour of pre-extrusion and finish extrusion. Because the gear teeth have been formed by the pre-extrusion, the purpose of the finish extrusion is for insufficient section compensation and tooth sizing. The load of finish extrusion is very low, so the workpiece does not need to be reheated.

Figure 12a shows the influence of the contour variation on the forming quality under the friction factor at 0.6. It reveals that with the increases of the contour variation, the height of the insufficient section is decreased. When the contour variation is 0.3 mm, the insufficient section is almost eliminated. Figure 12b shows the simulated result by using variable contour two-step warm extrusion when the contour variation is 0.3 mm. It is noted that the insufficient section is effectively compensated and the tooth filling is also improved.

Fig. 13 Experimental sample

Figure 13 shows the experimental sample. The accuracy of the finished gear is tested by using the coordinate measuring machine. The test standard is CAD model of spur gear with the theoretical parameters. Each gear tooth is measured by equivalently spaced 25 points. The mean deviation of each tooth is calculated through Eq. (6). The testing result is shown in Fig. 14; the maximum mean error of a single tooth is 15.5 μm. An example of the accuracy testing on one tooth is shown in Fig. 15; the maximum absolute error is 42.7 μm.

$$\overline{\delta} = \frac{\sum_{i=1}^{25} |\delta_i|}{25} \tag{6}$$

6 Conclusion

1. The deformation behavior of the $20Cr_2Ni_4A$ steel is coincident with the typical rules of the alloy steel. The true stress-strain curves integrally offset to the low stress area with the increase of the deformation temperature or the decrease of the strain rate. Nevertheless, one of the specific features of $20Cr_2Ni_4A$ steel is the softening mechanism gains rapidly to the upper hand at 973.15 K. The

Fig. 12 Variable contour two-step warm extrusion

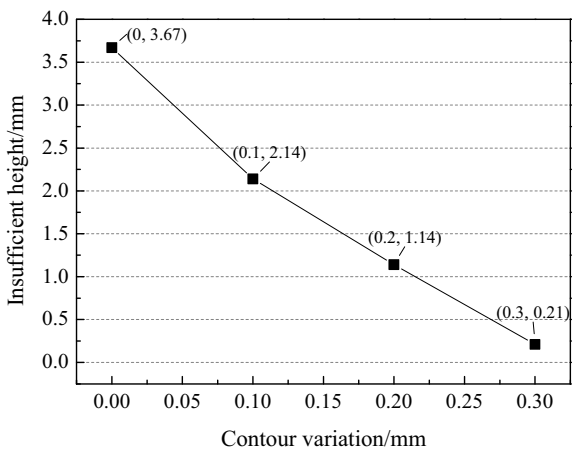

(A) Influence of contour variation on the forming quality

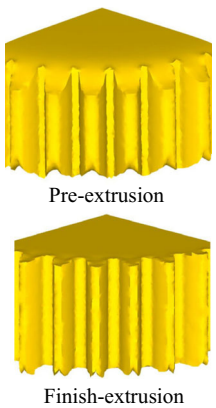

(B) Simulation result

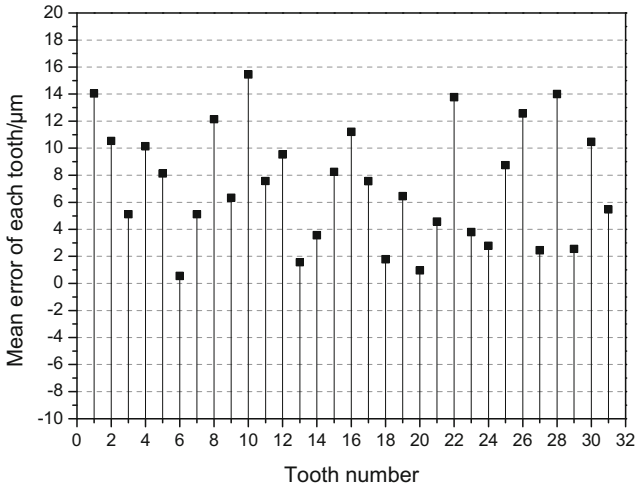

Fig. 14 Mean deviation of each tooth

Arrhenius-type constitutive equation with the Zener-Hollomon parameter for $20Cr_2Ni_4A$ steel at $\sigma_{0.3}$ could be expressed as follows:

$$\begin{cases} \sigma = 129.5906\ln\left\{\left(\dfrac{Z}{1.0859\times10^{7}}\right)^{1/5.148}+\left[\left(\dfrac{Z}{1.0859\times10^{7}}\right)^{2/5.148}+1\right]^{1/2}\right\} \\ Z=\dot{\varepsilon}\exp\left(\dfrac{190.96\times10^{3}}{8.314T}\right) \end{cases}$$

2. Lubricating condition, entrance angle, and initial blank size are the crucial factors of warm extrusion forming of spur gear. The insufficient section will be generated when the friction factor is greater than 0.5. Instead of the insufficient section, the addendum is elongated along the extrusion direction when the friction factor is less than 0.3. If the entrance angle is too large, the materials accumulation will occur during the gear tooth forming stage. The defect section will be worse if the straight section is too short.
3. The variable contour two-step warm extrusion is proposed to obtain a good forming result under a poor lubrication. Pre-extrusion is for the gear teeth formed, and finish extrusion is for insufficient section compensation and tooth sizing. With the increase of the contour variation, the height of the insufficient section is decreased. When the contour variation is 0.3 mm, the insufficient section is almost eliminated.

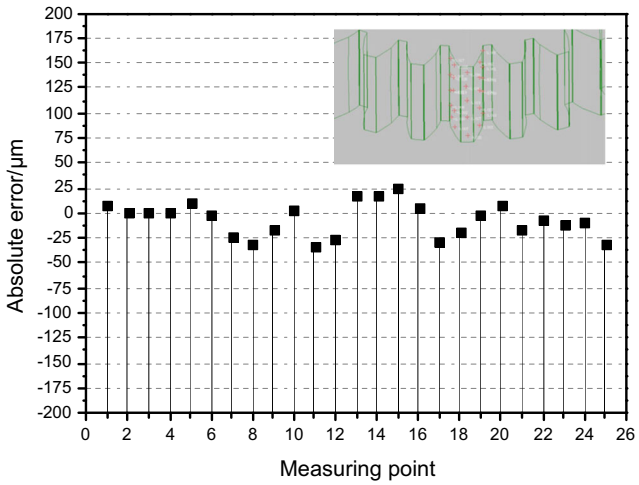

Fig. 15 Testing result of one tooth

Acknowledgments This work is supported by the Program for the Youth Top-notch Talents of Hebei Province.

References

1. Abdul NA, Dean TA (1986) An analysis of the forging of spur gear forms. Int J Mach Tool Des Res 26:113–123
2. Kondo K, Ohga K (1995) Precision cold die forging of a ring gear by divided flow method. Int J Mach Tools Manuf 35:1105–1113
3. Choi JC, Choi Y (1999) Precision forging of spur gears with inside relief. Int J Mach Tools Manuf 39:1575–1588
4. Cai J, Dean TA, Hu ZM (2004) Alternative die designs in net-shape forging of gears. J Mater Process Technol 150:48–55
5. Hu CL, Wang KS, Liu QK (2007) Study on a new technological scheme for cold forging of spur gears. J Mater Process Technol 187–188:600–603
6. Hu CL, Liu QK, Zhao Z, Chen J, Wu GM (2010) Two step forging process of spur gear based on rigid parallel motion. J Shanghai Jiaotong Univ (Sci) 15:241–244
7. Cheng FS, Hsu KK, Chen YS (2014) The study of hot forging process by using lower strength material as die. Mater Res Innov 18:22–25
8. Yang C, Zhao S, Zhang J (2014) Precision forging of spur gear by flow control forming method. Aust J Mech Eng 12:101–109
9. Dean TA (2000) The net-shape forming of gears. Mater Des 21: 271–278
10. Kawasaki K, Shinma K (2008) Design and manufacture of straight bevel gear for precision forging die by direct milling. Mach Sci Technol 12:170–182
11. Berviller L, Bigot R, Martin P (2006) Technological information concerning the integrated design of "net-shape" forged parts. Int J Adv Manuf Technol 31:247–257
12. Neugebauer R, Putz M, Hellfritzsch U (2007) Improved process design and quality for gear manufacturing with flat and round rolling. CIRP Ann Manuf Technol 56:307–312
13. Neugebauer R, Hellfritzsch U, Lahl M (2008) Advanced process limits by rolling of helical gears. Int J Mater Form 1:1183–1186
14. Zhang DW, Zhao SD (2014) New method for forming shaft having thread and spline by rolling with round dies. Int J Adv Manuf Technol 70:1455–1462
15. Zhu CD, Jiang X, Dai TL (2015) Research on technology of twin rollers rotary forging of spiral bevel gears. Ironmak Steelmak 42: 632–640
16. Han XH, Hua L, Zhuang WH, Zhang XC (2014) Process design and control in cold rotary forging of non-rotary gear parts. J Mater Process Technol 214:2402–2416
17. Li YY, Zhao SD, Fan SQ, Yan GH (2013) Study on the material characteristic and process parameters of the open-die warm

extrusion process of spline shaft with 42CrMo steel. J Alloys Compd 571:12–20
18. Jeong MS, Lee SK, Yun JH, Sung JH, Kim DH, Lee S, Choi TH (2013) Green manufacturing process for helical pinion gear using cold extrusion process. Int J Precis Eng Manuf 14:1007–1011
19. Yuan AF (2009) Cold extrusion of a long trapezium spline and its forming analysis. Int J Adv Manuf Technol 41:461–467
20. Song JH, Im YT (2007) The applicability of process design system for forward extrusion of spur gears. J Mater Process Technol 184: 411–419
21. Hu CL, Zhao Z, Gong AJ, Shi WB (2015) Study of an alternative novel cold forging process. Mater Manuf Process 30:1210–1217
22. Bingöl S, Ayer Ö, Altinbalik T (2015) Extrusion load prediction of gear-like profile for different die geometries using ANN and FEM with experimental verification. Int J Adv Manuf Technol 76:983–992
23. Jung SY, Kang MC, Kim C, Kim CH, Chang YJ, Han SM (2009) A study on the extrusion by a two-step process for manufacturing helical gear. Int J Adv Manuf Technol 41:684–693
24. Lin YC, Chen MS, Zhong J (2008) Effect of temperature and strain rate on the compressive deformation behavior of 42CrMo steel. J Mater Process Technol 205:308–315
25. Feng W, Fu YH (2014) High temperature deformation behavior and constitutive modeling for 20CrMnTiH steel. Mater Des 57:465–471